International Journal of Disaster Risk Reduction 98 (2023) 104124

Contents lists available at ScienceDirect

International Journal of Disaster Risk Reduction

journal homepage: www.elsevier.com/locate/ijdrr

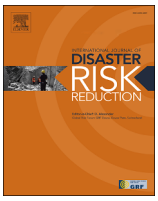

Post-earthquake fire ignition model uncertainty in regional probabilistic shaking–fire cascading multi-hazard risk assessment: A study of earthquakes in Japan

Tomoaki Nishino

Disaster Prevention Research Institute, Kyoto University, Gokasho, Uji, Kyoto, 611-0011, Japan

ARTICLE INFO

Keywords:
Fire following earthquake
Cascading disaster
Ignition rate
Epistemic uncertainty
Hierarchical Bayesian model
Multi-hazard risk assessment

ABSTRACT

Fires following earthquakes have significant impact on urban communities in earthquake-prone countries with wooden buildings, in addition to the main earthquake hazard of ground shaking. Regional-scale post-earthquake fire risk assessments are important for developing effective risk reduction strategies. Such risk assessments require the consideration of epistemic uncertainty, that is, uncertainty caused by lack of knowledge concerning the best models, in addition to aleatoric uncertainty. This study focused on epistemic uncertainty in post-earthquake fire ignition estimations, and incorporated it into risk assessments by using alternative empirical ignition models. The key objectives of this study were as follows: (1) correlating the probability of ignition per person to the ground motion intensity based on data for different past large earthquakes in Japan; (2) investigating the impact of using ignition models calibrated on different earthquake events in risk assessments through a realistic case study considering possible large earthquakes. A hierarchical Bayesian Poisson regression analysis revealed that the empirical relationship between the ignition probability and ground motion intensity greatly varies across six major large earthquakes in Japan from 1995 to 2022. Particularly, the effects of ignition prevention measures that have been widely implemented in households since the 1995 Kobe earthquake were inferred from much smaller ignition probabilities in approximately the last 10 years. The effects of this high epistemic uncertainty manifested as the large variability of the loss exceedance curve for a portfolio of buildings. These results indicate that the new ignition models can help to foster risk-informed decision-making under epistemic uncertainty.

1. Introduction

Fires following earthquakes are a type of cascading earthquake hazard, and can cause catastrophic damage to urban environments, particularly in areas with densely constructed wooden buildings in earthquake-prone countries [1]. Historical large earthquakes have triggered simultaneous outbreaks of multiple fires in urban areas, resulting in conflagrations by overwhelming firefighting capabilities. The fires following the 1923 Kanto earthquake, which struck the Tokyo–Yokohama metropolitan area, Japan, on September 1 (11:58 a.m. local time) with a magnitude of 7.9, are the most notable post-earthquake fire event in history owing to the extremely large fire damage to buildings and loss of life [2]. In Tokyo, the capital city of Japan, 98 fires started simultaneously at different locations after the earthquake, and eventually destroyed an area of approximately 34.7 km^2, including over 210,000 buildings, and killed over 58,000 people [2]. Numerous fire ignitions occurred because the earthquake struck approximately at noon, when numerous open flames were being used for cooking [2]. Additionally, the fires spread easily to adjacent buildings because numerous

E-mail address: nishino.tomoaki.3c@kyoto-u.ac.jp.

https://doi.org/10.1016/j.ijdrr.2023.104124
Received 8 June 2023; Received in revised form 30 October 2023; Accepted 2 November 2023
Available online 4 November 2023

wooden buildings were densely built in the city, and a strong wind with a speed of approximately 10 m/s was blowing from the beginning of the event until the next morning [2]. Such low urban fire resistance and bad weather conditions, combined with simultaneous multiple ignitions, enhanced the fire development.

In the last 100 years following the 1923 Kanto earthquake, various measures have been taken in Japan to enhance the urban fire resistance and fire service strength. These include the formation of firebreaks with roads and fire-resistant buildings to prevent fire from spreading, zoning to regulate the structure of buildings in designated areas, improvement of areas with closely spaced wooden buildings, promotion of fire-resistant buildings and wooden buildings with fire protection for exterior walls, openings, and roofs, and improvement of fire stations, pump trucks, and water sources [3]. These efforts contributed to the development of modern Japanese society, wherein urban conflagrations are rare events. Nevertheless, the 1995 Kobe earthquake, which struck Kobe, Japan, and its surrounding area with a magnitude of 7.3, triggered 269 fires, resulting in the burning of over 7000 buildings [4]. This earthquake highlights that post-earthquake fire risk still exists in Japan. Therefore, Japan places strong emphasis on understanding the risk of post-earthquake fires to develop effective policies and strategies for risk reduction, similar to other earthquake-prone countries [5–12] and particularly countries with many wooden buildings, such as the United States and New Zealand.

Because various post-earthquake fire scenarios are probable owing to uncertainties, such as the number and location of ignitions and the wind velocity and direction, post-earthquake fire risk assessments typically adopt probabilistic approaches to incorporate this aleatoric uncertainty [5,13–17]. Particularly, historical post-earthquake ignition rate data have been analyzed to randomly generate multiple simultaneous ignitions for future earthquake events, as reviewed in Ref. [5]. This ignition model enables probabilistic loss estimations using fire spread and suppression models [13], where the randomly sampled time sequences of weather parameter values from observation data are occasionally used [16,17]. Such probabilistic assessments considering aleatoric uncertainty provide a better foundation for fire risk reduction planning compared with deterministic assessments, which are limited to specific scenarios, such as the worst-case scenario, and cannot provide information on the variability of fire losses and frequency. However, the incorporation of epistemic uncertainty, that is, uncertainty caused by lack of knowledge concerning the best model, is also important in risk assessments, because risk assessments vary greatly depending on the model used [18,19]. For example, in probabilistic seismic hazard and risk assessments, epistemic uncertainty is typically considered using logic tree approaches, where several alternative models are set as branches for hazard/risk components, such as the earthquake rate models, ground motion prediction equations, and seismic fragility functions, and weights are assigned to each alternative model [20–25]. Specifically, epistemic uncertainty is considered by evaluating a group of weight-assigned hazard/risk curves based on several alternative model combinations.

Similar to seismic hazard and risk assessments, post-earthquake fire risk assessments comprise several components, such as the ignition and fire spread models, and must therefore consider epistemic uncertainty as long as there are alternative models for such components. Particularly, the uncertainty of ignition models, which are linked to fire spread models to numerically simulate the development of simultaneous fires in urban areas, can be notable, because numerous ignition models have been proposed since 2000 [26–35] (earlier models are summarized in Ref. [5]). With the exceptions of fault-tree ignition models [26,30], all available ignition models are regression models, which typically correlate the probability of ignition per floor area or person to the ground motion intensity, based on data for past large earthquakes. This empirical relationship may greatly vary among earthquake events because ignition mechanisms are affected by societal changes such as built environment and lifestyle changes. As an example, most ignitions following the 1923 Kanto earthquake resulted from cooking appliances using open flames [2], such as the *kamado* and *shichirin*, while the 1995 Kobe earthquake caused ignitions related to electrical appliances, gas appliances, and oil heaters [36]. Since the 1995 Kobe earthquake, several large earthquakes, such as the 2011 Tohoku and 2016 Kumamoto earthquakes, have also caused numerous ignitions, similar to the 1923 Kanto and 1995 Kobe earthquakes. Moreover, prevention measures for ignitions resulting from gas appliances and oil heaters have been widely implemented in households. Specifically, automatic gas shut-off devices, which sense shaking and immediately cut off gas flow, are now built into almost all the household gas meters in Japan. Similarly, seismically sensitive oil heaters equipped with automatic turn-off devices are now common in Japan. This widespread implementation can change the occurrence probability of post-earthquake fires.

Therefore, this study investigated post-earthquake fire ignition model uncertainty, and incorporated it into post-earthquake fire risk assessment. Although many areas around the world are prone to post-earthquake fires, this study focused on Japan without considering other countries, because country-specific conditions exist. Specifically, an empirical study specific to Japan was undertaken. Nevertheless, the methodology adopted in this study is applicable to other countries and may enable comparison among countries. The main objectives of this study were as follows: (1) investigate the variability of the empirical relationship between the probability of ignition per person and ground motion intensity among past large earthquakes (i.e., investigate the inter-event variability of empirical ignition models); (2) investigate the impact of using ignition models calibrated on different earthquake events on post-earthquake fire risk estimates for possible large earthquakes. Fig. 1 illustrates the technical flow diagram of the process used in this study to achieve the above-mentioned objectives. First, this study focused on six major large earthquakes that occurred in Japan from 1995 to 2022, developed post-earthquake fire ignition datasets, and conducted Poisson regressions using a hierarchical Bayesian modeling approach, which can analyze group differences in regressions. Then, the ignition model uncertainty was considered using a logic tree, that is, the developed empirical ignition models were incorporated as alternative models with equal weights into a multi-hazard risk assessment framework for ground shaking and post-earthquake fires [17]. Finally, this study conducted a realistic case study for Kyoto, Japan, which is a historical city with densely constructed wooden buildings, and evaluated a group of weight-assigned loss exceedance curves at the regional scale. Notably, the case study focused on direct economic losses for a building portfolio, but did not consider indirect economic losses and losses of human life, because the adopted framework is not capable of evaluating such losses. However, the loss of life can be evaluated by linking the framework to urban post-earthquake fire evacuation models [37].

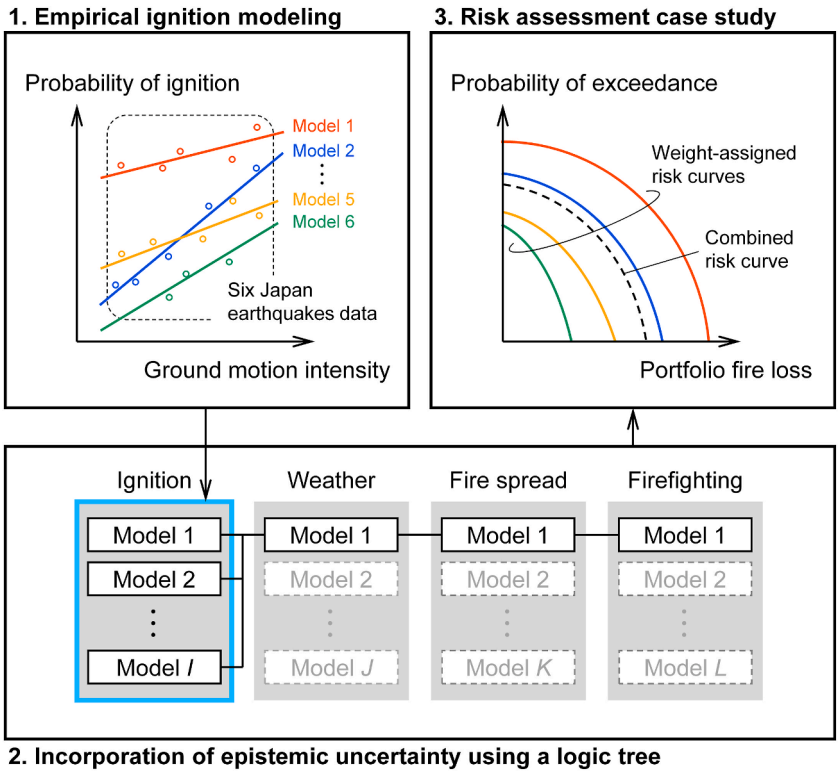

Fig. 1. Technical flow diagram of process used to investigate post-earthquake fire ignition model uncertainty and incorporate it into risk assessments.

The rest of this paper is organized as follows. Section 2 defines the post-earthquake fires of interest, presents the data and formulation of the empirical ignition models, and discusses the regression analysis results. Section 3 presents the shaking–fire multi-hazard risk assessment through a case study, and discusses the impact of the ignition model uncertainty. Finally, Section 4 presents the conclusions drawn from this study and discusses the scope of future work.

2. Empirical modeling of post-earthquake fire ignition

The post-earthquake fires of interest are defined as building fires that occur up to 72 h after a large earthquake as a consequence of ground shaking, such as fires caused by damage to, moving of, and overturning of goods and equipment, and by electrical power restorations. Therefore, despite their post-earthquake occurrence, fires that are strongly related to human factors rather than ground shaking, such as fires caused by candles providing light inside buildings during a blackout, are not included in the post-earthquake fire definition of this study.

In this study, empirical post-earthquake fire ignition modeling correlates the number of ignition incidents following a large earthquake to the ground motion intensity and the exposed population using a Poisson distribution, similar to previous studies [34,38]. Specifically, the ignition probability per person is modeled as a function of the ground motion intensity. The reasons for this are as follows: (1) the number of people living in an area represents human activity levels, which are related to the probability of fire occurrence; (2) spatial demographic data are generally available. Although the type of human activity in the area is not considered, the number of people living in the area is occasionally used to capture the macroscopic characteristics of post-earthquake fire ignitions [34,39]. Alternatively, a building-floor-area-based modeling approach may be more appropriate; however, little information is available on nationwide spatiotemporal floor area distributions.

This Poisson regression ignition modeling requires dividing the ground motion intensity into bins, and counting the number of ignition incidents and exposed population corresponding to each bin. Three types of ground motion intensity measures are considered to determine which intensity measure is the most effective in improving the predictions. These intensity measures are the peak ground acceleration (PGA), peak ground velocity (PGV), and Japan Meteorological Agency seismic intensity (JMA intensity). In this study, the PGA and PGV are measured in cm/s^2 and cm/s units, respectively, while the JMA intensity, which is typically calculated from three-component acceleration waveforms by applying specific filters, does not have a physical unit. The JMA intensity is divided into intensity unit intervals of 0.4, while the PGA and PGV are divided such that they approximately correspond to the JMA intensity bins with consideration of their empirical relationships with the JMA intensity [40].

A hierarchical Bayesian approach was adopted to estimate the model parameters using data obtained from different earthquake events. Specifically, the objective was to investigate how the empirical relationship between the ignition probability and ground motion intensity varies across different earthquake events. The approach can handle data wherein observations are grouped by one or

more categorical variables. Each model parameter is treated as a random variable for which a probability distribution represents the degrees of belief in the values, and its prior distribution is updated using data based on Bayes' theorem. Some model parameters are allowed to vary based on group differences by considering their prior distributions as dependent on other parameters, which are also assigned prior distributions.

2.1. Data

Data from six major large earthquakes in Japan from 1995 to 2022 were analyzed to investigate the inter-event variability of post-earthquake fire ignition models. These earthquakes are the 1995 Kobe, 2011 Tohoku, 2016 Kumamoto (foreshock and mainshock), 2018 Hokkaido, and 2022 Fukushima earthquakes; the source information is listed in Table 1. The 1995 Kobe and 2011 Tohoku earthquakes were selected from the three earthquakes in Japanese history that are associated with great earthquake disasters (the third one is the 1923 Kanto earthquake). The remaining earthquakes were selected from destructive earthquakes that occurred in the last 10 years and completely destroyed more than 200 houses. These earthquakes are representative of recent earthquakes that have produced strong ground motions over a large area of the built environment, and allow the development of ignition models applicable to large accelerations or velocities of interest in risk assessments. Although Japan has historically suffered from post-earthquake fires, events before 1995, such as the 1923 Kanto and 1948 Fukui earthquakes, were not considered owing to the difficulty of knowing the ground motion intensity distribution and exposed population, which are required for ignition modeling. As previously stated, ignition sources for fires following historical earthquakes [2], such as traditional cooking appliances using open flames, are different to those for fires following recent earthquakes [36,41,42], such as electrical appliances, gas appliances, and oil heaters, owing to lifestyle differences. Therefore, the exclusion of such events appears to have a minor effect on the scope of this study and practical risk assessment. Because nationwide dense seismic observation networks had not yet been established in Japan, the ground motion intensity distributions for the 1995 Kobe earthquake were estimated based on Yamaguchi and Yamazaki [43]. Their method calculates the ground motion intensities backward from survey data on the district-level building damage ratios using empirical seismic fragility functions. Therefore, the estimated ground motion intensity distributions for the 1995 Kobe earthquake are limited to areas included in the survey. The ground motion intensity distributions for the earthquakes from 2011 to 2022 are provided by a quick estimation system called QuiQuake [44], which produces maps displaying the ground motion intensities based on records observed by nationwide strong-motion seismograph networks operated by the National Research Institute for Earth Science and Disaster Resilience of Japan. This system first calculates the intensities on hard rock under seismic stations by removing the site amplification effect; then, it spatially interpolates the intensities by considering the attenuation characteristics from the source, and finally calculates the intensities on the ground surface at 250 m intervals by considering the site amplification effect.

Post-earthquake fires are identified from the records obtained from fire departments, which include information concerning the fire type, location (address), date and time of occurrence, and ignition source. The fire records for the 1995 Kobe, 2011 Tohoku, and 2016 Kumamoto (foreshock and mainshock) earthquakes have been previously reported [36,41,42]. This study collected the fire records for the 2018 Hokkaido and 2022 Fukushima earthquakes from municipal fire departments through questionnaire surveys. Among the included fire incidents, fires that do not meet the above-mentioned post-earthquake fire definition are excluded, while fires whose ignition sources are unknown are included. Then, the fires that can be linked to the ground motion intensity based on their location are considered.

The identified post-earthquake fires are 166 fires associated with the 1995 Kobe earthquake, 114 fires associated with the 2011 Tohoku earthquake, 4 fires associated with the 2016 Kumamoto earthquake (foreshock), 6 fires associated with the 2016 Kumamoto earthquake (mainshock), 5 fires associated with the 2018 Hokkaido earthquake, and 10 fires associated with the 2022 Fukushima earthquake. Although there is a small number of post-earthquake fire observations for some earthquake events, these observations still allow the development of ignition models for the pertinent earthquake events, because the hierarchical Bayesian modeling approach described below can function with limited data by estimating models referring to tendencies in other groups with many observations. As an example, Fig. 2 overlays the post-earthquake fire locations on the estimated PGV distributions for the six earthquakes. The overlay links each post-earthquake fire to the PGV and enables the counting of the number of ignition incidents that fall within each PGV bin. Notably, only areas subjected to the PGV of 5 cm/s or more are shown. Among the earthquakes, there are remarkable differences in the extent of exposure to high PGV. The 500 m grid population data are also overlaid on the estimated PGV distributions to count the population that falls within each PGV bin. The same applies to the other intensity measures. Consequently, the number of ignition incidents and exposed population are obtained for all intensity measures with specific bins, as shown in Fig. 3. These datasets are used for the hierarchical Bayesian Poisson regressions described in the following sections. As previously stated, the

Table 1
Six major large earthquakes in Japan considered in empirical post-earthquake fire ignition modeling; source information provided by Japan Meteorological Agency.

ID	Name	Magnitude	Time (JST)	Location	Depth
A	1995 Kobe earthquake	M7.3	1995-01-17 05:46	34°35.9′N 135°02.1′E	16 km
B	2011 Tohoku earthquake	Mw9.0	2011-03-11 14:46	38°06.2′N 142°51.6′E	24 km
C	2016 Kumamoto earthquake (foreshock)	M6.5	2016-04-14 21:26	32°44.5′N 130°48.5′E	11 km
D	2016 Kumamoto earthquake (mainshock)	M7.3	2016-04-16 01:25	32°45.2′N 130°45.7′E	12 km
E	2018 Hokkaido earthquake	M6.7	2018-09-06 03:07	42°41.4′N 142°00.4′E	37 km
F	2022 Fukushima earthquake	M7.4	2022-03-16 23:36	37°41.8′N 141°37.3′E	57 km

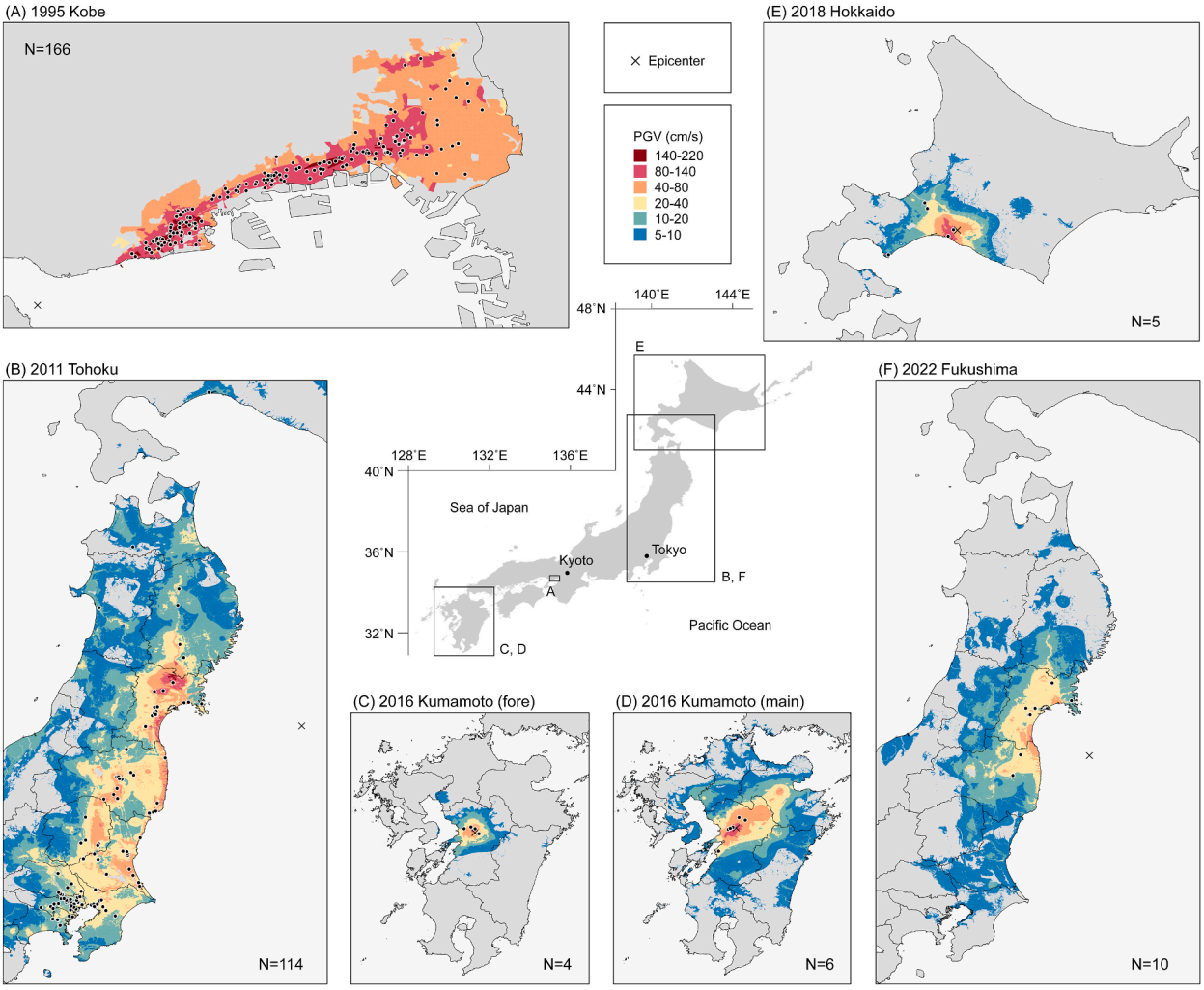

Fig. 2. Estimated PGV distributions and post-earthquake fire locations for six major large earthquakes in Japan.

PGA and PGV bins are specified such that they approximately correspond to the JMA intensity bins, which are specified in the range of 4.4–7.2 at intervals of 0.4; therefore, the PGA and PGV bin widths are not identical.

Fig. 4 compares the ignition source breakdowns among the earthquakes. The cross table highlights that electricity-related fires, that is, fires related to electrical appliances, equipment, and wiring, account for most post-earthquake fires in approximately the last 10 years (from 2011 to 2022), while conventional ignition sources, such as gas appliances and oil heaters, have rarely caused fires in approximately the last 10 years, although some fires are related to open flames. Most fires following the 1995 Kobe earthquake had unknown causes; however, they may have included numerous ignitions resulting from gas appliances and oil heaters, because prevention measures for ignitions resulting from gas appliances and oil heaters, such as seismically sensitive household gas meters and oil heaters with automatic turn-off devices (as described in Section 1), may not have been as widespread among households at that time as they have become in recent years.

Only the fire records for the 2018 Hokkaido and 2022 Fukushima earthquakes include information concerning occupant firefighting. Even if a combustible object inside a building is ignited, a fire may be extinguished by occupants during its initial stages without developing into a fire involving the entire building. Fig. 5 shows the percentages of the ignition incidents where occupants attempted and succeeded in firefighting during the initial stages. The rates of occupant firefighting attempt and success are 50%–60% and 30%–40%, respectively. For comparison, the rate of occupant firefighting success has been reported as 20.4% for fires following the 1995 Kobe earthquake [45]. For the 2018 Hokkaido earthquake, two ignition incidents wherein occupants did not attempt firefighting were caused by electrical appliance and firewood or charcoal; one ignition incident wherein occupants attempted but did not succeed in firefighting was caused by high-temperature objects. For the 2022 Fukushima earthquake, five ignition incidents wherein occupants did not attempt firefighting were caused by electrical equipment and wiring; two ignition incidents wherein occupants attempted but did not succeed in firefighting were caused by electrical wiring. Owing to limited data, a clear relationship between the ignition source and attempted or successful occupant firefighting is not observed.

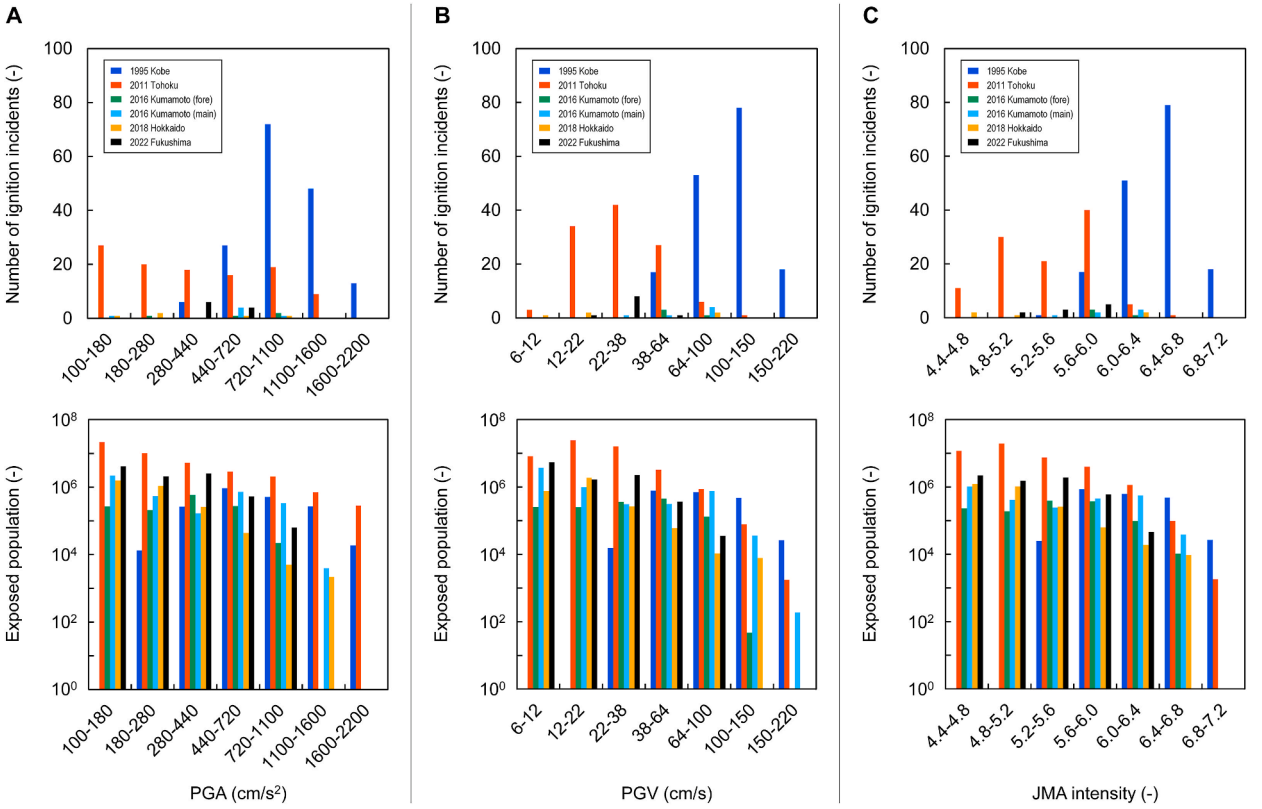

Fig. 3. Datasets used for empirical post-earthquake fire ignition modeling: number of ignition incidents and exposed population for specific ground motion intensity bins.

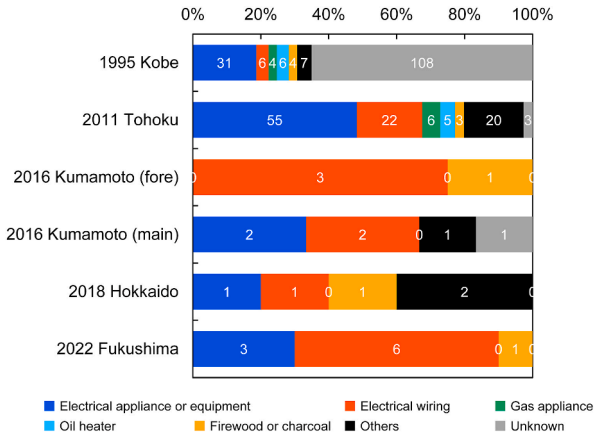

Fig. 4. Post-earthquake fire ignition source breakdowns for six major large earthquakes in Japan.

2.2. Formulation

Let p be the probability of ignition per person. Considering that p is not negative, the logarithm of p is modeled as a function of the ground motion intensity x:

$$\ln p = a + b \ln x \tag{1}$$

for the PGA and PGV, and

$$\ln p = a + bx \tag{2}$$

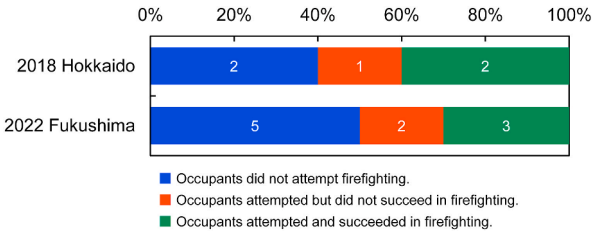

Fig. 5. Rates of occupant firefighting attempt and success for fires following the 2018 Hokkaido and 2022 Fukushima earthquakes.

for the JMA intensity, where a is the intercept and b is the slope. In contrast to the JMA intensity ranging up to approximately 7, the PGA and PGV are on the order of 100–1000 cm/s^2 and 10–100 cm/s, respectively. Therefore, the PGA and PGV models take the logarithm of x to harmonize with the JMA intensity model.

The probability of y ignition incidents occurring for n persons living in an area subjected to ground motion with intensity x is assumed to have a Poisson distribution, as follows:

$$f(y|\lambda) = \frac{\lambda^y \exp(-\lambda)}{y!} \tag{3}$$

where $\lambda(=np)$ is the average number of ignition incidents.

Thus, the logarithm of λ can be expressed by a linear relationship as

$$\ln \lambda = \ln n + a + b \ln x \tag{4}$$

for the PGA and PGV, and

$$\ln \lambda = \ln n + a + bx \tag{5}$$

for the JMA intensity, where the logarithm of the exposed population $\ln n$ is considered as an offset term.

Following a hierarchical Bayesian approach [46], each model parameter is divided into a parameter common to all earthquake events and a parameter specific to each earthquake event representing an unexplained variation from the common parameter value. Hereinafter, i is used to identify the earthquake events. The intercept and slope of the i-th earthquake event are modeled as follows:

$$a_i = c_a + r_{a,i} \tag{6}$$

$$b_i = c_b + r_{b,i} \tag{7}$$

where c_a and c_b are parameters common to all earthquake events, and $r_{a,i}$ and $r_{b,i}$ are parameters specific to the i-th earthquake event.

2.3. Bayesian inference setup

Let D be a dataset of the number of ignition incidents y versus the ground motion intensity x linked to the exposed population n. Because, as mentioned above, the number of ignition incidents and exposed population are counted for the specific ground motion intensity bins, the intensity bin medians are used as the value of x. Hereinafter, j is used to identify the intensity bins. The probability of dataset D being obtained can be written as the product of the Poisson distributions for all earthquake events and all intensity bins:

$$p\left(D|c_a, c_b, r_{a,1}, \cdots, r_{a,K}, r_{b,1}, \cdots, r_{b,K}\right) = \prod_{i=1}^{K}\prod_{j=1}^{L} \frac{\lambda_{ij}^{y_{ij}} \exp\left(-\lambda_{ij}\right)}{y_{ij}!} \tag{8}$$

where $K(=6)$ is the number of earthquake events, and $L(=7)$ is the number of intensity bins.

Based on Bayes' theorem, the posterior distribution can be written as

$$\text{Posterior} \propto p\left(D|c_a, c_b, r_{a,1}, \cdots, r_{a,K}, r_{b,1}, \cdots, r_{b,K}\right) \times \text{Prior} \tag{9}$$

therefore, the prior distribution must be specified [46].

For the common parameter c_a, a non-informative prior distribution [46] is specified. Because c_a can take any positive or negative value, a normal distribution with a mean of zero and standard deviation of 100 was adopted as its prior distribution. In Bayesian statistics, this distribution is typically used as a sufficiently flat probability distribution. The same applies to the other common parameter c_b. Specifically, the prior distributions are set as follows:

$$c_a \sim \text{Normal}(0, 100), \quad c_b \sim \text{Normal}(0, 100) \tag{10}$$

For the event-specific parameter $r_{a,i}$, a prior distribution is not specified for each earthquake event individually. Instead, a hierarchical prior distribution [46], which can change the overall variation, is specified to handle all earthquake events simultaneously. More

specifically, the prior distribution of $r_{a,i}$ is first set as a normal distribution with a mean of zero and standard deviation s_a. Then, the prior distribution of this hyperparameter s_a is specified. Because s_a can take any positive value, a uniform distribution in the range of 0–1000, as a non-informative prior distribution, was adopted as the prior distribution of s_a [47]. In Bayesian statistics, this distribution is typically used as a sufficiently flat probability distribution. The same applies to the other event-specific parameter $r_{b,i}$. Specifically, the prior distributions are set as follows:

$$\left.\begin{array}{l} r_{a,i} \sim \text{Normal}\left(0, s_a\right) \\ s_a \sim \text{Uniform}\left(0, 1000\right) \end{array}\right], \quad \left.\begin{array}{l} r_{b,i} \sim \text{Normal}\left(0, s_b\right) \\ s_b \sim \text{Uniform}\left(0, 1000\right) \end{array}\right] \tag{11}$$

Hence, the posterior distribution can be written as follows [46]:

$$\begin{aligned} &p\left(c_a, c_b, s_a, s_b, r_{a,1}, \cdots, r_{a,K}, r_{b,1}, \cdots, r_{b,K} | D\right) \\ &\propto p\left(D | c_a, c_b, r_{a,1}, \cdots, r_{a,K}, r_{b,1}, \cdots, r_{b,K}\right) p\left(c_a\right) p\left(c_b\right) p\left(s_a\right) p\left(s_b\right) \prod_{i=1}^{K} p\left(r_{a,i} | s_a\right) \prod_{i=1}^{K} p\left(r_{b,i} | s_b\right) \end{aligned} \tag{12}$$

The posterior distribution is determined using the Markov chain Monte Carlo method [48]. Specifically, Markov chains are used to generate samples from the distribution of the product of the prior and likelihood, and samples identified as having converged to the equilibrium distribution are substituted for the posterior distribution. Four Markov chains with different starting values are constructed using Hamiltonian Monte Carlo sampling [49] in the Stan software [50] to monitor that they converge to similar posterior distributions. Each chain generates 6000 samples. The first 3000 samples that appear to depend on a starting value are removed, and the remaining 3000 samples are kept. Therefore, a total of 12,000 samples are adopted to determine the posterior distribution. The Gelman–Rubin statistic $\hat{R}$ [51] is used for convergence diagnosis. The conventional threshold value for $\hat{R}$ is 1.1 [51]; that is, the posterior distribution is considered to be convergent when all values for $\hat{R}$ are below 1.1.

2.4. Results and discussion

To discuss the results obtained from Bayesian inference, this study focused on the posterior distribution medians and compared the models adopting them as parameter values with the data. Table 2 lists the posterior distribution medians. All values for the $\hat{R}$ statistic are below 1.1, and very close to 1; therefore, it can be considered that the generated samples converge. Notably, the models compute very small ignition probabilities per person; however, they can produce multiple simultaneous fires when highly populated cities are subjected to strong ground motion.

Fig. 6 compares the models adopting the posterior distribution medians as parameter values with the data. The data points represent the ratios of the number of ignition incidents to the exposed population for the specific ground motion intensity bins; therefore, data points are not plotted for the bins wherein the number of ignition incidents or exposed population is zero. The inferred models highlight the large variability among the earthquakes with positive correlations between the ignition probability per person and ground motion intensity for all adopted intensity measures. Considering the PGV-based models as an example, and considering the model for the 2011 Tohoku earthquake, which computes the medium ignition probabilities and has sufficient sample sizes, as a reference model, the inter-event variations of the ignition probability range from approximately 0.37-fold to 9.29-fold increases. Particularly, while earthquake models in approximately the last 10 years vary with lower ignition probabilities, the model for the 1995 Kobe earthquake alone computes much higher ignition probabilities compared with the other models. A possible major factor contributing to this remarkable difference is the change of the ignition sources. As previously stated, prevention measures for ignitions resulting from gas appliances and oil heaters, such as seismically sensitive household gas meters and oil heaters with automatic turn-off devices, may not have been as widespread at the time of the 1995 Kobe earthquake as they have become in recent years. The widespread implementation of ignition prevention measures may have successfully reduced the number of ignition incidents following earthquakes in approximately the last 10 years. Even though the ignition probabilities appear to have converged to a similar level

Table 2
Bayesian-inferred post-earthquake fire ignition model parameter values: posterior distribution medians.

Parameter	Earthquake	PGA		PGV		JMA intensity	
		Median	$\hat{R}$	Median	$\hat{R}$	Median	$\hat{R}$
a	1995 Kobe	−22.81662	1.0001	−18.85483	1.0004	−23.16649	1.0006
	2011 Tohoku	−18.70230	1.0004	−18.11251	1.0005	−22.59432	1.0006
	2016 Kumamoto (foreshock)	−23.32464	1.0001	−18.96443	1.0006	−23.32625	1.0004
	2016 Kumamoto (mainshock)	−22.45616	0.9999	−19.15477	1.0017	−23.36919	1.0001
	2018 Hokkaido	−23.13921	1.0003	−18.71696	1.0004	−23.13722	1.0000
	2022 Fukushima	−24.26935	1.0000	−18.94663	1.0002	−23.38099	1.0009
b	1995 Kobe	2.00147	1.0001	2.11409	1.0005	2.19810	1.0006
	2011 Tohoku	1.02589	1.0004	1.56327	1.0004	1.83815	1.0006
	2016 Kumamoto (foreshock)	1.76675	1.0001	1.68222	1.0006	1.90328	1.0004
	2016 Kumamoto (mainshock)	1.52915	0.9999	1.59088	1.0013	1.83291	1.0002
	2018 Hokkaido	1.81641	1.0003	1.80239	1.0003	1.95662	0.9999
	2022 Fukushima	1.86782	1.0000	1.73404	1.0002	1.91711	1.0007

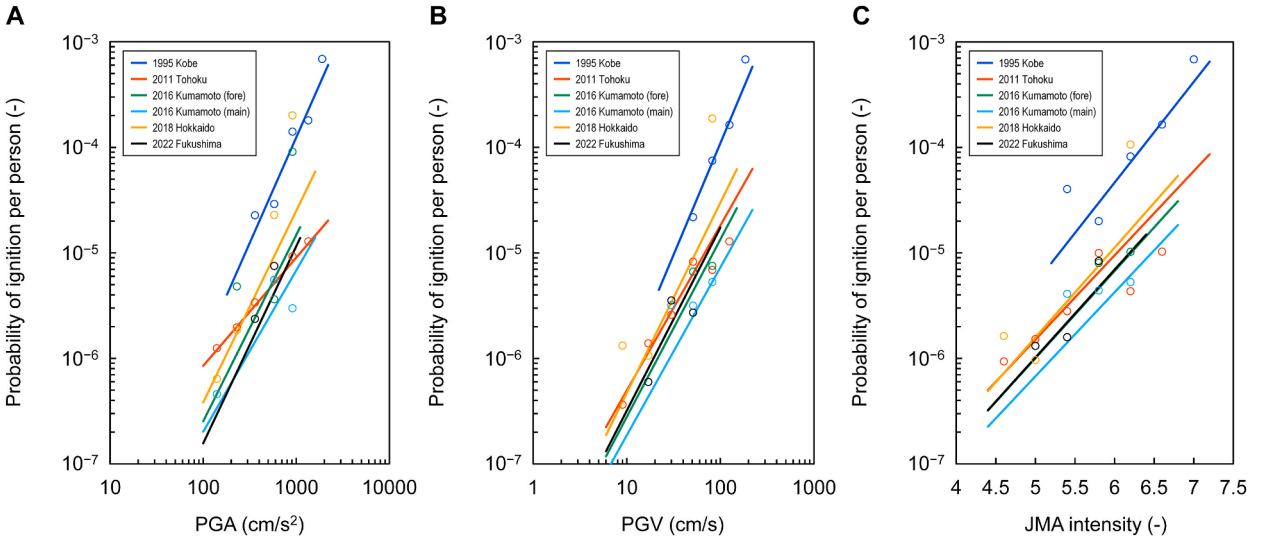

Fig. 6. Bayesian-inferred post-earthquake fire ignition models and their comparison with data; the models adopt the posterior distribution medians as parameter values.

in approximately the last 10 years, the model selection is likely to have significant impact on post-earthquake fire risk estimates, because the inter-event variations are not negligible, even in approximately the last 10 years. Therefore, ignition model uncertainty must be incorporated into post-earthquake fire risk assessments. This aspect is addressed in the next section.

In addition to the inter-event variability, the intensity measure selection can also be considered to improve the predictions. However, model selections based on typical information criteria, such as the widely applicable information criterion [52], are not available because the data for each intensity measure are different. Therefore, this study considered the difference between the predicted average number of ignition incidents λ_{pre} and the observed number of ignition incidents y_{obs} for a given earthquake event and a given intensity bin as the residual, and assumed that an intensity measure that achieves a higher reduction of the root mean square of the residuals (RMSR) for all earthquake events and all intensity bins enables better predictions. Specifically, the RMSR is defined as

$$\mathrm{RMSR} = \sqrt{\frac{1}{KL}\sum_{i=1}^{K}\sum_{j=1}^{L}\left(\lambda_{ij,pre} - y_{ij,obs}\right)^2} \tag{13}$$

and computed for each intensity measure by comparing the model predictions to the observations (Fig. 7). Unexpectedly, the PGV-based models produce the smallest RMSR with a value of 2.60. Therefore, the PGV is the most effective explanatory variable compared with the PGA (RMSR = 4.63) and JMA intensity (RMSR = 3.83). Considering that the PGA and JMA intensity correspond to the earthquake response spectra in a period range of zero and 0.1–1 s, respectively [53], it is reasonable to expect that the PGA or JMA intensity is more effective because post-earthquake fire ignitions are strongly related to the seismic response of goods and equipment (mainly in low-rise and mid-rise buildings), which are sensitive to such short-period ground motions. However, the results contradict this expectation, and identifying the underlying physical causes of these findings requires further research. Fig. 7 indicates that the residuals for the 1995 Kobe and 2011 Tohoku earthquakes, which have the first and second largest number of ignition obser-

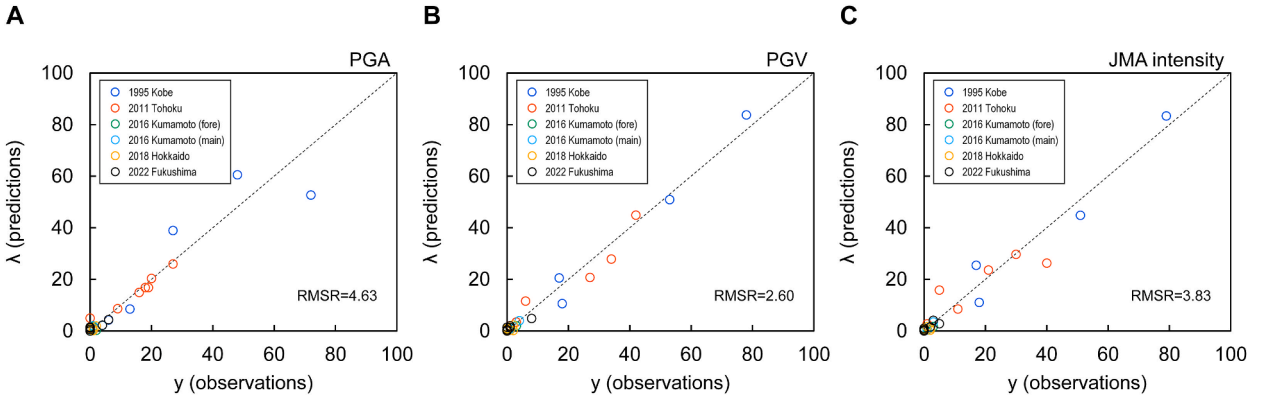

Fig. 7. Observed number of ignition incidents versus predicted average number of ignition incidents.

vations, dominate the RMSR. Specifically, the PGA cannot effectively explain the data for the 1995 Kobe earthquake owing to the residuals of up to 19.3, and the JMA intensity cannot effectively explain the data for the 2011 Tohoku earthquake owing to the residuals of up to 13.7. In contrast, the PGV can effectively explain the data for both the 1995 Kobe and 2011 Tohoku earthquakes owing to the smaller residuals of up to 7.4 and 6.2, respectively, and thus achieves a larger reduction of the RMSR compared with the other intensity measures.

3. Shaking–fire multi-hazard risk assessment

A multi-hazard risk assessment for ground shaking and post-earthquake fires was conducted with consideration to the post-earthquake fire ignition model uncertainty. Specifically, equal weights were assigned to several ignition models as alternative models, and a group of weight-assigned loss exceedance curves was evaluated for a building portfolio using a shaking–fire multi-hazard risk assessment framework [17]. Then, the curves were combined into a single loss exceedance curve. In other words, a combination of different ignition models with equal weights was used in the development of the loss exceedance curve. Here, three ignition models were selected from the PGV-based models, which can provide better predictions compared with models based on other intensity measures. Specifically, the models for the 1995 Kobe, 2011 Tohoku, and 2016 Kumamoto (mainshock) earthquakes were selected to compute the largest, medium, and smallest ignition probabilities among the new ignition models, respectively. Similar to a previous study [17], this case study was conducted for the historical city of Kyoto, Japan, based on national seismic activity models [54]. Six modeled earthquakes along major active faults were considered (Fig. 8). These earthquake models specify a single moment magnitude (Mw) and the probability of its occurrence for each specified source fault. The essential points of the case study are (1) the variability in the total number of ignitions across the entire city depending on the ignition models, and (2) the variability in the loss exceedance curve for a portfolio of buildings in Nishijin and its surrounding area, which is a designated high-priority area with densely constructed wooden buildings, depending on the ignition models. The city-scale ignition analysis used a 500 m grid population exposure

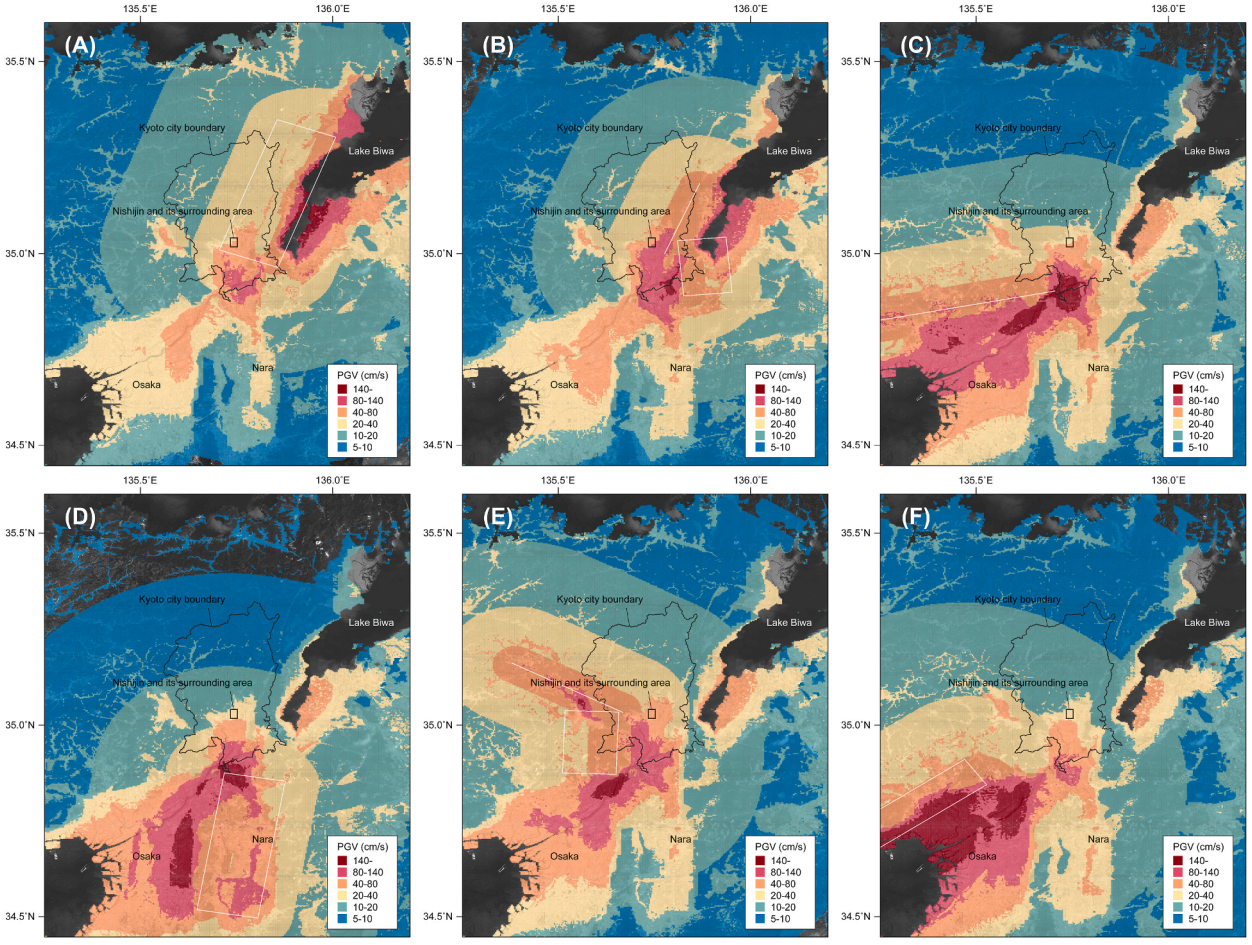

Fig. 8. Domains for city-scale ignition and neighborhood-scale loss analyses, specified source faults selected from national seismic activity models of Japan [54], and distributions of average PGVs predicted by ground motion prediction equation [55]: (a) Biwako Seigan fault of Mw 6.9 earthquake; (b) Hanaore fault of Mw 6.9 earthquake; (c) Arima-Takatsuki fault of Mw 7.1 earthquake; (d) Ikoma fault of Mw 6.9 earthquake; (e) Kyoto Nishiyama fault of Mw 7.0 earthquake; (f) Rokko-Awaji fault of Mw 7.3 earthquake. The probability of occurrence can be found in the literature [17].

model, while the neighborhood-scale loss analysis used an additional detailed building exposure model [17], which contains information on the spatially distributed buildings, such as the building location, footprint, construction type, number of floors, thermal properties of the exterior walls, and area of the exterior wall openings.

3.1. Methodology

The shaking–fire multi-hazard risk assessment framework [17] is an extension of probabilistic seismic risk assessments that includes a post-earthquake fire model consisting of the ignition, weather, urban fire spread, and fire brigade response models. This framework can evaluate the exceedance probability of direct economic losses for a portfolio of buildings, as a result of the combined effect of ground shaking and post-earthquake fires, in a predefined future time period by comprehensively considering various earthquake- and fire-related uncertainties through Monte Carlo simulations. This risk is defined as the probability $p(L \geq l;t)$ of the total loss L for the portfolio of buildings, caused by the combined effect of ground shaking and post-earthquake fires, exceeding a certain value l at least once within t years when all possible earthquakes are considered. This definition is expressed as follows:

$$p\left(L \geq l;t\right) = 1 - \prod_{k} \left[1 - p\left(E_k;t\right) p\left(L \geq l \middle| E_k\right)\right] \tag{14}$$

where $p(E_k;t)$ is the probability of the k-th earthquake occurring within t years, and $p\left(L \geq l \middle| E_k\right)$ is the probability of the total loss L exceeding a certain value l when the k-th earthquake occurs. Equation (14) ignores the probability of earthquakes occurring more than once within t years, because earthquake recurrence intervals are typically much longer than the time period of interest t. Aftershocks are not considered, potentially resulting in an underestimation of the risk.

While the earthquake occurrence probability $p(E_k;t)$ is evaluated from historical records and geological and geographical data, the conditional loss exceedance probability $p\left(L \geq l \middle| E_k\right)$ can be numerically evaluated through Monte Carlo simulations, as follows:

$$p\left(L \geq l \middle| E_k\right) = \frac{1}{n_{MCS}} \sum_{j=1}^{n_{MCS}} I\left(L_j \geq l \middle| E_k\right) \tag{15}$$

where n_{MCS} is the number of Monte Carlo trials, and $I(\cdot)$ is the indicator function that takes the value of 1 when the total loss for the j-th trial L_j is greater than or equal to l; otherwise, it takes the value of 0.

The total loss for the j-th trial L_j can be evaluated by considering the replacement cost of buildings, as follows:

$$L_j = \sum_{i=1}^{n_{bldg}} L_{ij} = \sum_{i=1}^{n_{bldg}} \max\left(L_{S,ij}, L_{F,ij}\right) = \sum_{i=1}^{n_{bldg}} \left[C_{R,i} \times \max\left(LR_{S,ij}, LR_{F,ij}\right)\right] \tag{16}$$

where n_{bldg} is the number of buildings; L_{ij}, $L_{S,ij}$, and $L_{F,ij}$ are the losses resulting from the combined effect of ground shaking and post-earthquake fires, ground shaking alone, and post-earthquake fires alone, respectively, for the i-th building and j-th trial; $C_{R,i}$ is the total replacement cost of the i-th building; $LR_{S,ij}$ and $LR_{F,ij}$ are the loss ratios for the ground shaking and post-earthquake fires, respectively. The shaking loss ratio must be determined by considering different damage states, such as complete damage and partial damage. The fire loss ratio can be determined by considering two damage states, complete damage or no damage, because post-earthquake fires in low-rise wooden buildings typically affect the entire building. Hence, Equation (16) takes the greater of the shaking loss or fire loss, as opposed to the cumulative effect.

The model implementation for evaluating the above equations is as follows. (1) The fault location and geometry, Mw, and occurrence probability are specified for individual earthquakes using the national seismic activity models of Japan [54]. (2) The PGVs at the building locations are stochastically evaluated using an up-to-date empirical ground motion prediction equation for Japan [55]. This equation includes correction terms for the site amplification caused by deep sedimentary layers and shallow soft soils; these terms are evaluated using nationwide shear-wave velocity structure models [56]. (3) The damage states resulting from ground shaking (completely destroyed and semi-destroyed) are stochastically evaluated for individual buildings using empirical seismic fragility functions [43,57,58], and the ground shaking loss ratios to the total replacement costs are evaluated. Similar to Goda and Risi [18], a combination of three seismic fragility functions for Japanese low-rise wooden buildings is used in the Monte Carlo simulations to incorporate the fragility function uncertainty into the assessments. (4) The ignition probabilities are evaluated for individual buildings using the new empirical ignition models, and the fire-starting buildings are stochastically determined. Specifically, the ignition models compute the ignition probability per person; therefore, this probability is converted to the ignition probability per building, which enables the stochastic determination of the fire-starting buildings by generating a uniform random number between 0 and 1 for each building and comparing it with the ignition probability. Buildings for which the generated random number is equal to or less than the ignition probability are considered as the fire-starting buildings. (5) The time histories of the weather parameters, including the outdoor air temperature and wind velocity and direction, are randomly sampled from one-year hourly weather data obtained at a given meteorological station. (6) The fire brigade response times are stochastically evaluated for individual fire outbreaks using the empirical distribution of the time from outbreak to detection for the 1995 Kobe earthquake [36], which has a sufficient sample size for high ground motion intensity levels. (7) The time-varying behaviors of urban fire spread are numerically simulated using a physics-based urban fire spread model [59] under the stochastically determined ignition, weather, and fire brigade response conditions, and the post-earthquake fire loss ratios to the total replacement costs are evaluated for individual buildings. Fig. 9 shows examples of the post-earthquake urban fire spread simulations for Nishijin and its surrounding area, adopting 72 h as the simulation period. These ex-

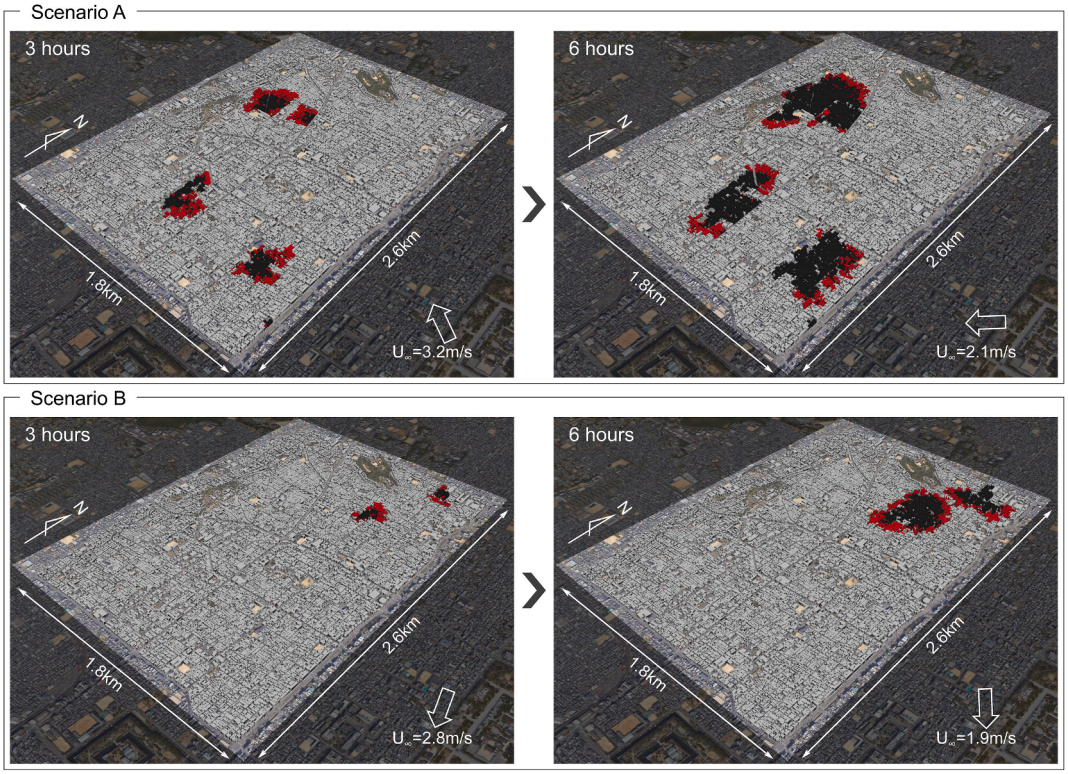

Fig. 9. Examples of post-earthquake urban fire spread simulations for Nishijin and its surrounding area with densely constructed wooden buildings (visualized on Google Earth): gray, red, and black objects represent unburned, burning, and burned buildings, respectively. (For interpretation of the references to colour in this figure legend, the reader is referred to the Web version of this article.)

amples demonstrate that the stochastic multi-hazard modeling can successfully generate various post-earthquake fire scenarios with a different number of fires, fire-starting buildings, and wind velocity and direction. One similarity is that the simulated fires simultaneously start at multiple locations, with an enlarged burned area, and begin to burn out in sequence closer to the fire-starting buildings. Thus, they form belt-like burning regions along the fire fronts. Additional details concerning the implemented models can be found in the literature [17].

3.2. Results and discussion

Fig. 10 shows the empirical cumulative distribution functions of the total number of ignitions obtained from the city-scale analysis of 600 trials for each ignition model, focusing on the Hanaore fault earthquake. As expected, the different ignition models obtained remarkably different results. Specifically, the effect of significant decreases in the ignition probability in approximately

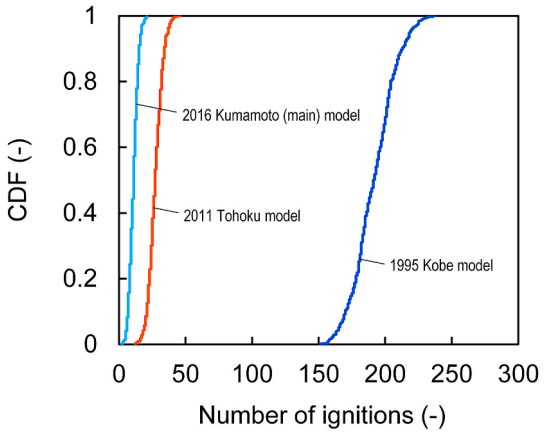

Fig. 10. Empirical cumulative distribution functions of total number of ignitions obtained through city-scale analysis under Hanaore fault earthquake using different post-earthquake fire ignition models.

the last 10 years manifests as a great reduction in the number of fire occurrences compared with the predictions using the ignition model for the 1995 Kobe earthquake. The total number of ignitions is in the range of 2–237. The predictions of the six new ignition models fall within this wide range because the ignition models for the 1995 Kobe and 2016 Kumamoto (mainshock) earthquakes compute the largest and smallest ignition probabilities, respectively. Notably, because numerous PGV distributions are stochastically generated as a result of the error term included in the ground motion prediction equation, there is greater variation in the total number of ignitions than when using the average PGV distribution. However, this intra-model variation appears to be smaller than the inter-model variation.

Fig. 11 shows the building portfolio loss exceedance curves obtained from the neighborhood-scale analysis of 600 trials for each ignition model. Unsurprisingly, using different ignition models significantly affects the risk estimates. Specifically, the ignition model for the 1995 Kobe earthquake provides larger fire loss exceedance probabilities compared with using a combination of all ignition models. Conversely, the ignition models for the 2011 Tohoku and 2016 Kumamoto (mainshock) earthquakes provide smaller fire loss exceedance probabilities compared with using a combination of all ignition models. Considering a 0.5% probability of exceedance in 50 years, using the ignition model for the 1995 Kobe earthquake increases the loss estimate by approximately 3.2 and 25.6 times compared with using the ignition models for the 2011 Tohoku and 2016 Kumamoto (mainshock) earthquakes, respectively. This highlights that the careful selection of post-earthquake fire ignition models is important in post-earthquake fire risk assessments. Specifically, given the possibility that some ignition prevention measures have successfully reduced the ignition probability since the 1995 Kobe earthquake, it may be reasonable to use ignition models for earthquakes that occurred in approximately the last 10 years in risk assessments for future earthquakes. However, the uncertainty is not negligible even in the ignition models for recent earthquakes. Therefore, it is preferable to use a combination of these models. Another important point is that all fire loss exceedance curves lie below the shaking loss exceedance curve at small total losses, while this relationship is reversed at large total losses. This indicates that typical earthquake risk assessments that consider ground shaking alone may significantly underestimate the loss exceedance probabilities. Particularly, such assessments may ignore the rare but catastrophic effects of post-earthquake fires.

4. Conclusions

This study developed empirical post-earthquake fire ignition models based on data for six major large earthquakes in Japan from 1995 to 2022 using hierarchical Bayesian Poisson regression, and investigated the impact of the ignition model uncertainty on regional risk estimates through a realistic case study considering possible large earthquakes. The key findings of this study are as follows. (1) The empirical relationship between the ignition probability per person and ground motion intensity greatly varies across different earthquakes. (2) The effects of ignition prevention measures that have been widely implemented in households since the 1995 Kobe earthquake are inferred from much smaller ignition probabilities in approximately the last 10 years. (3) The PGV is the most effective intensity measure for explaining the ignition data, as opposed to the PGA and JMA intensity. (4) Using different ignition models has a significant impact on the risk assessment results. (5) The new ignition models serve as alternative models for incorporating epistemic uncertainty into risk assessment.

The findings of this study contribute to the advancement of regional shaking–fire multi-hazard risk assessment. However, the results were obtained from empirical and case studies specific to Japan and cannot be generalized to different countries and future events. Therefore, further investigations are needed. Particularly, the ignition models developed in this study are based on data for past large earthquakes, but the built environment and lifestyles are expected to change continuously in the future. Because it is impos-

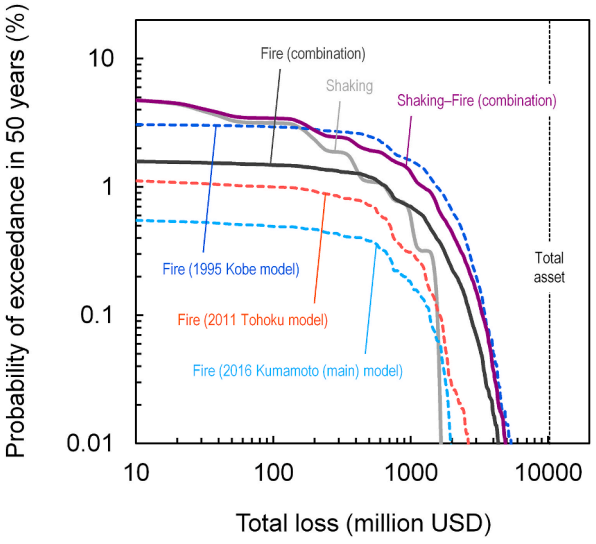

Fig. 11. Loss exceedance curves of building portfolio obtained through neighborhood-scale analysis using different post-earthquake fire ignition models.

sible to clarify the timeframe over which the models developed in this study remain valid, it is necessary to assess the relationship between the ignition probability and the ground motion intensity whenever a large earthquake occurs in the future, and update the ignition models to reflect the latest situation. Additionally, epistemic uncertainty in other components, such as the weather, building exposure, and urban fire spread models, was not addressed in this study, and should be investigated in future work. Incidentally, preventing electricity-related ignitions is important for further reducing post-earthquake fire risk. Seismic circuit breakers, which are household devices that detect shaking and automatically cut off the electrical power, are increasingly receiving attention in Japan as a low-cost and fast post-earthquake fire risk reduction measure, as opposed to conventional structural measures, such as retrofitting or rebuilding to improve fire resistance. To promote the adoption of seismic circuit breakers, the associated risk reduction effects depending on the implementation rate must be quantified. Therefore, further work is needed to improve the management of post-earthquake fire risk.

Funding

This study was supported by the Core-to-Core Collaborative Research Program (2023-K-1-2-8) of the Earthquake Research Institute at The University of Tokyo, and the Disaster Prevention Research Institute at Kyoto University, funded by the Ministry of Education, Culture, Sports, Science, and Technology (MEXT) of Japan under The Second Earthquake and Volcano Hazards Observation and Research Program (Earthquake and Volcano Hazard Reduction Research).

Declaration of competing interest

The author declares that he has no known competing financial interests or personal relationships that could have appeared to influence the work reported in this paper.

Data availability

Derived data supporting the findings of this study are available from the corresponding author upon reasonable request.

Acknowledgements

The author is grateful to municipal fire departments that completed the questionnaire. The author also thanks Edanz for the English editing of a draft of this manuscript.

References

[1] N.E. Khorasani, M. Garlock, Overview of fire following earthquake: historical events and community responses, International Journal of Disaster Resilience in the Built Environment 8 (2) (2017) 158–174.
[2] C. Scawthorn, T. Nishino, J.C. Schencking, J. Borland, Kantō daikasai: the great Kantō fire following the 1923 earthquake, Bull. Seismol. Soc. Am. 113 (2023) 1902–1923.
[3] Y. Murosaki, Large fire measures, Chapter 21 of the Handbook of fire, in: Japan Association of Fire Science and Engineering, Kyoritsu Shuppan, Tokyo, Japan, 1997, pp. 1393–1449 (in Japanese).
[4] Fire and Disaster Management Agency, Confirmed Report on the Great Hanshin Earthquake, 2006. https://www.fdma.go.jp/disaster/info/assets/post1.pdf. (Accessed 2 May 2023).
[5] S. Lee, R. Davidson, N. Ohnishi, C. Scawthorn, Fire following earthquake—reviewing the state-of-the-art of modeling, Earthq. Spectra 24 (2008) 933–967.
[6] C. Scawthorn, Fire following earthquake aspects of the Southern San Andreas fault Mw 7.8 earthquake scenario, Earthq. Spectra 27 (2011) 419–441.
[7] G. Thomas, D. Heron, J. Cousins, M. Roiste, Modeling and estimating post-earthquake fire spread, Earthq. Spectra 28 (2012) 795–810.
[8] P. Baquedano Julia, T.M. Ferreira, H. Rodrigues, Post-earthquake fire risk assessment of historic urban areas: a scenario-based analysis applied to the Historic City Centre of Leiria, Portugal, Int. J. Disaster Risk Reduc. 60 (2021) 102287.
[9] P. Gulum, E. Ayyildiz, A.T. Gumus, A two level interval valued neutrosophic AHP integrated TOPSIS methodology for post-earthquake fire risk assessment: an application for Istanbul, Int. J. Disaster Risk Reduc. 61 (2021) 102330.
[10] M. Coar, A. Sarreshtehdari, M. Garlock, N.E. Khorasani, Methodology and challenges of fire following earthquake analysis: an urban community study considering water and transportation networks, Nat. Hazards 109 (2021) 1–31.
[11] C. Scawthorn, Fire following earthquake—the potential in Istanbul, in: S. Akkar, A. Ilki, C. Goksu, M. Erdik (Eds.), Advances in Assessment and Modeling of Earthquake Loss, Springer Tracts in Civil Engineering. Springer, Cham, 2021.
[12] Z. He, N.E. Khorasani, Identification and hierarchical structure of cause factors for fire following earthquake using data mining and interpretive structural modeling, Nat. Hazards 112 (2022) 947–976.
[13] Technical Council on Lifeline Earthquake Engineering, in: C. Scawthorn, J.M. Eidinger, A.J. Schiff (Eds.), Fire Following Earthquake, American Society of Civil Engineers, Technical Council for Lifeline Earthquake Engineering, Reston, Virginia, 2005.
[14] C. Scawthorn, Fire following earthquake aspects of the Southern San Andreas fault Mw 7.8 earthquake scenario, Earthq. Spectra 27 (2011) 419–441.
[15] J. Cousins, G. Thomas, D. Heron, W. Smith, Probabilistic modeling of post-earthquake fire in Wellington, New Zealand, Earthq. Spectra 28 (2012) 553–571.
[16] T. Nishino, T. Tanaka, A. Hokugo, An evaluation method for the urban post-earthquake fire risk considering multiple scenarios of fire spread and evacuation, Fire Saf. J. 54 (2012) 167–180.
[17] T. Nishino, Probabilistic urban cascading multi-hazard risk assessment methodology for ground shaking and post-earthquake fires, Nat. Hazards 116 (2023) 3165–3200.
[18] K. Goda, R.D. Risi, Multi-hazard loss estimation for shaking and tsunami using stochastic rupture sources, Int. J. Disaster Risk Reduc. 28 (2018) 539–554.
[19] S. Matsushima, Core-to-core collaborative research between earthquake Research Institute, the University of Tokyo and disaster prevention Research Institute, Kyoto University during FY2014 to FY2018, J. Disaster Res. 15 (2020) 187–201.
[20] H. Crowley, J. Bommer, R. Pinho, J. Bird, The impact of epistemic uncertainty on an earthquake loss model, Earthq. Eng. Struct. Dynam. 34 (2005) 1653–1685.
[21] W. Marzocchi, M. Taroni, J. Selva, Accounting for epistemic uncertainty in PSHA: logic tree and ensemble modeling, Bull. Seismol. Soc. Am. 105 (4) (2015) 2151–2159.
[22] J. Selva, R. Tonini, I. Molinari, M.M. Tiberti, F. Romano, A. Grezio, D. Melini, A. Piatanesi, R. Basili, S. Lorito, Quantification of source uncertainties in seismic probabilistic tsunami hazard analysis (SPTHA), Geophys. J. Int. 205 (2016) 1780–1803.
[23] V. Silva, Uncertainty and correlation in seismic vulnerability functions of building classes, Earthq. Spectra 35 (4) (2019) 1515–1539.
[24] P. Kalakonas, V. Silva, A. Mouyiannou, A. Rao, Exploring the impact of epistemic uncertainty on a regional probabilistic seismic risk assessment model, Nat.

Hazards 104 (2020) 997–1020.
[25] E. Field, K. Milner, K. Porter, Assessing the value of removing earthquake-hazard-related epistemic uncertainties, exemplified using average annual loss in California, Earthq. Spectra 36 (4) (2020) 1912–1929.
[26] R. Williamson, N. Groner, Ignition of Fires Following Earthquakes Associated with Natural Gas and Electric Distribution Systems. Pacific Earthquake Engineering Research Center Report, University of California, Berkeley, CA, 2000.
[27] A. Ren, X. Xie, The simulation of post-earthquake fire-prone area based on GIS, J. Fire Sci. 22 (2004) 421–439.
[28] S. Zhao, L. Xiong, A. Ren, A spatial-temporal stochastic simulation of fire outbreaks following earthquake based on GIS, J. Fire Sci. 24 (2006) 313–339.
[29] C. Scawthorn, Enhancements in HAZUS-MH, fire following earthquake task 3: updated ignition equation, Technical Report, PBS&J and the National Institute of Building Sciences, SPA Risk LLC, USA, 2009, pp. 1–91.
[30] M.R. Zolfaghari, E. Peyghaleh, G. Nasirzadeh, Fire following earthquake, intra-structure ignition modeling, J. Fire Sci. 27 (2009) 45–79.
[31] R.A. Davidson, Modeling postearthquake fire ignitions using generalized linear (mixed) models, J. Infrastruct. Syst. 15 (2009) 351–360.
[32] D. Anderson, R.A. Davidson, K. Himoto, C. Scawthorn, Statistical modeling of fire occurrence using data from the Tohoku, Japan Earthquake and Tsunami, Risk Anal. 36 (2016) 378–395.
[33] N.E. Khorasani, T. Gernay, M. Garlock, Data-driven probabilistic post-earthquake fire ignition model for a community, Fire Saf. J. 94 (2017) 33–44.
[34] T. Nishino, A. Hokugo, A stochastic model for time series prediction of the number of post-earthquake fire ignitions in buildings based on the ignition record for the 2011 Tohoku earthquake, Earthq. Spectra 36 (2020) 232–249.
[35] Q. Tong, T. Gernay, A hierarchical Bayesian model for predicting fire ignitions after an earthquake with application to California, Nat. Hazards 111 (2022) 1637–1660.
[36] K. Suzuki, Y. Matsubara, Fires for 10 days after the 1995 Kobe earthquake, Report of National Research Institute of Fire and Disaster 49 (1995) 21–30 (in Japanese).
[37] T. Nishino, T. Tanaka, S. Tsuburaya, Development and validation of a potential-based model for city evacuation in post-earthquake fires, Earthq. Spectra 29 (2013) 911–936.
[38] T. Nishino, Probabilistic analysis of the vulnerability of fire departments to ignitions following megathrust earthquakes in the Nankai Trough subduction zone, Japan, Fire Saf. J. 120 (2021) 103038.
[39] A. Sekizawa, K. Sasaki, Study on fires following the 2011 Great East-Japan earthquake based on the questionnaire survey to fire departments in affected areas, Fire Saf. Sci. 11 (2014) 691–703.
[40] S. Midorikawa, K. Fujimoto, I. Muramatsu, Correlation of new J.M.A. instrumental seismic intensity with former J.M.A. seismic intensity and ground motion parameters, Journal of Social Safety Science 1 (1999) 51–56 (in Japanese).
[41] Japan Association for Fire Science and Engineering, Report on Fires Following the 2011 Great East Japan Earthquake. Fires following the Great East Japan earthquake. (2016) 1–36 (Chapter 3).
[42] K. Suzuki, M. Shinohara, Summary of fires in the 2016 Kumamoto earthquake and countermeasures, Report of National Research Institute of Fire and Disaster 122 (2017) 11–17 (in Japanese).
[43] N. Yamaguchi, F. Yamazaki, Estimation of strong motion distribution in the 1995 Kobe earthquake based on building damage data, Earthq. Eng. Struct. Dynam. 30 (2001) 787–801.
[44] National Institute of Advanced Industrial Science and Technology, QuiQuake: Quick Estimation System for Earthquake Map Triggered by Observed Records, 2013. https://gbank.gsj.jp/QuiQuake/index.en.html. (Accessed 6 February 2023).
[45] Architectural Institute of Japan, Fire damage and civil activities. Damage to information systems (1998) Report on the Hanshin-Awaji Earthquake Disaster p.54 (in Japanese).
[46] A. Gelman, J.B. Carlin, H.S. Stern, D.B. Dunson, A. Vehtari, D.B. Rubin, Bayesian Data Analysis, third ed., Chapman & Hall/CRC Press, New York, US, 2013.
[47] A. Gelman, Prior distributions for variance parameters in hierarchical models, Bayesian Analysis 1 (3) (2006) 515–533.
[48] N. Metropolis, A. Rosenbluth, M. Rosenbluth, M. Teller, E. Teller, Equations of state calculations by fast computing machines, J. Chem. Phys. 21 (6) (1953) 1087–1092.
[49] R. Neal, in: S. Brooks, A. Gelman, G. Jones, X. Meng (Eds.), MCMC Using Hamiltonian Dynamics, Chapter 5 of the Handbook of Markov Chain Monte Carlo, Chapman & Hall/CRC Press, Boca Raton, US, 2011, pp. 116–162.
[50] Stan Development Team, Stan Modeling Language: User's Guide and Reference Manual, 2016, version 2.14.0. https://mc-stan.org. (Accessed 2 May 2023).
[51] A. Gelman, D.B. Rubin, Inference from iterative simulation using multiple sequences, Stat. Sci. 7 (4) (1992) 457–472.
[52] S. Watanabe, Asymptotic equivalence of Bayes cross validation and widely applicable information criterion in singular learning theory, J. Mach. Learn. Res. 11 (2010) 3571–3594.
[53] Y. Sakai, S. Koyama, Knowledge on seismic response of buildings and damage, in: Earthquake Ground Motion and Strong Motion Prediction: Key Items for Learning the Basics, first ed., Architectural Institute of Japan, 2016, pp. 213–236 (in Japanese).
[54] N. Morikawa, H. Fujiwara, Updates to the seismic activity models of Japan: lessons from the Great Tohoku earthquake, Seismol Res. Lett. 87 (6) (2016) 1259–1264.
[55] N. Morikawa, H. Fujiwara, A new ground motion prediction equation for Japan applicable up to M9 mega-earthquake, J. Disaster Res. 8 (2013) 878–888.
[56] Japan Seismic Hazard Information Station (J-SHIS), National Research Institute for Earth Science and Disaster Resilience, 2019, https://doi.org/10.17598/nied.0010.
[57] S. Midorikawa, Y. Ito, H. Miura, Vulnerability functions of buildings based on damage survey data of earthquakes after the 1995 Kobe earthquake, Journal of Japan Association for Earthquake Engineering 11 (2011) 34–47 (in Japanese).
[58] H. Wu, K. Masaki, K. Irikura, S. Kurahashi, Empirical fragility curves of buildings in northern Miyagi Prefecture during the 2011 off the Pacific coast of Tohoku earthquake, J. Disaster Res. 11 (2016) 1253–1270.
[59] T. Nishino, Physics-based urban fire spread simulation coupled with stochastic occurrence of spot fires, Stoch. Environ. Res. Risk Assess. 33 (2019) 451–463.